Benchmark of gyrokinetic, kinetic MHD and gyrofluid codes for the linear calculation of fast particle driven TAE dynamics

メタデータ	言語: English 出版者: 公開日: 2021-12-22 キーワード (Ja): キーワード (En): 作成者: Könies, Axel, BRIGUGLIO, S., GORELEKOV, Nikolai, Fehér, T., ISAEV, M., LAUBER, PH., MISHCHENKO, Alexey, SPONG, Donald A., TODO, Yasushi, COOPER, Wilfred A., HATZKY, Roman, Kleiber, Ralf, BORCHARDT, M., VLAD, G., BIANCALANI, Alessandro, BOTTINO, A., ITPA, EP TG メールアドレス: 所属:
URL	http://hdl.handle.net/10655/00012824

This work is licensed under a Creative Commons Attribution-NonCommercial-ShareAlike 3.0 International License.

Benchmark of gyrokinetic, kinetic MHD and gyrofluid codes for the linear calculation of fast particle driven TAE dynamics

A. Könies,[1, a)] S. Briguglio,[2] N. Gorelenkov,[3] T. Fehér,[4] M. Isaev,[5] Ph. Lauber,[4] A. Mishchenko,[1] D. A. Spong,[6] Y. Todo,[7] W. A. Cooper,[8] R. Hatzky,[4] R. Kleiber,[1] M. Borchardt,[1] G. Vlad,[2] A. Biancalani,[4] A. Bottino,[4] and ITPA EP TG

[1)] *Max Planck Institute for Plasma Physics, Wendelsteinstr. 1, 17491 Greifswald, Germany*

[2)] *ENEA C. R. Frascati, Via E. Fermi 45, CP 65-00044 Frascati, Italy*

[3)] *Princeton Plasma Physics Laboratory, Princeton University, Princeton, New Jersey 08543, USA*

[4)] *Max Planck Institute for Plasma Physics, Boltzmannstr. 2, 85748 Garching, Germany*

[5)] *NRC Kurchatov Institute, 123182 Moscow, Russia*

[6)] *Oak Ridge National Laboratory, Oak Ridge, Tennessee, USA*

[7)] *National Institute for Fusion Science, 322-6 Oroshi-cho, Toki 509-5292, Japan*

[8)] *École Polytechnique Fédérale de Lausanne, Swiss Plasma Center, CH1015 Lausanne, Switzerland*

(Dated: 25 September 2018)

Fast particles in fusion plasmas may drive Alfvén modes unstable leading to fluctuations of the internal electromagnetic fields and potential loss of particles. Such instabilities can have an impact on the performance and the wall-load of machines with burning plasmas such as ITER. A linear benchmark for a toroidal Alfvén eigenmode (TAE) is done with 11 participating codes with a broad variation in the physical as well as the numerical models. A reasonable agreement of around 20% has been found for the growth rates. Also, the agreement of the eigenfunctions and mode frequencies is satisfying. however, they are found to depend strongly on the complexity of the used model.

[a)] Electronic mail: axel.koenies@ipp.mpg.de

I. INTRODUCTION.

Fast particles in ITER may originate from the fusion process itself or from external heating, such as Neutral Beam Injection (NBI). It is well known that those non-thermal populations of fast particles may interact with otherwise stable Alfvén waves in the bulk plasma driving them unstable[1,2]. This process takes place as a resonance phenomenon that requires a kinetic treatment of the fast particles but not necessarily a kinetic treatment of the bulk plasma. The oscillating electro-magnetic field in the plasma may lead to a loss of supra-thermal particles. As a consequence, damage to in-vessel components of the machine is possible.
In the last decades, much effort has been invested in the development of theory and codes that can be used to describe and explain the related phenomena. However, up to now, there is no well-understood standard case that these models have been tested against quantitatively. After studying mode damping, by providing the first comprehensive quantitative code comparison for the fast particle drive, the ITPA Energetic particle Topical Group is contributing to the design activity of the ITER operation scenario[3]. The benchmark of different codes and models for the energetic ion driven modes is necessary for evaluating the accuracy of their predictions. Prior to an application to the plasma behavior in ITER, the international benchmarking effort between a variety of codes shall ensure scientific quality and reliability when predictions for ITER are made.
In this paper, we present a comprehensive benchmark of different gyrokinetic and hybrid MHD-gyrokinetic codes on the linear dynamics of the toroidicity-induced Alfén Eigenmode (TAE). This international benchmark was originally introduced in Ref. 4, and the complete list of results is shown here.

II. THEORY

As it has been outlined in the previous section, a kinetic description of fast particles or an appropriate closure of the fluid equations is necessary. In this section, different physical models in different implementations are described.

A. MHD/kinetic hybrid approach

Historically, the waves have been obtained from ideal MHD theory while the interaction with the wave has been treated with a drift or gyro-kinetic model. There are different levels

of sophistication to couple both models. In the following we will address the hole class as "MHD/kinetic hybrid" models.

If the calculation is done perturbatively, the linear drift- or gyro-kinetic equation for the fast particles is solved in the given field of a pre-calculated MHD wave. The growth rate is calculated from the power transfer of the particles in relation to the energy stored in the mode. Linear versions of this model are the NOVA-K[6], CAS3D-K[5], CKA-EUTERPE[11], VENUS[12] and AE3D-K[9].

It is interesting to note but not a topic of this paper that the perturbative model can be generalized to a non-linear version. Then, the mode structure is also a pre-calculated MHD eigenfunction but their phase and amplitude can change in time[7,8].

In some codes, the kinetic equation is solved with a particle-in-cell (PIC) method. Here, numerical marker particles are distributed in phase space and represent a large number of real particles. As the gyro-kinetic equation is of first order, it can be solved using the method of characteristics, i.e. by following particle orbits. PIC codes have advantages in difficult geometries such as stellarators but noise issues have to be properly addressed. A widely used method is the so-called δf model where the distribution function is split into a background distribution function f_0 which is usually a function of the constants of the unperturbed motion and a perturbation δf. An insightful description can be found in Ref. 13. While it is straight-forward to implement orbit losses in a full f simulation, it can be tricky for δf codes (see below).

The Tables I and II summarize the most important properties of the perturbative kinetic MHD codes participating in the benchmark.

code	MHD code	PIC	FOW	FLR	reference
NOVA-K	NOVA	no	2nd order	J_0	6
VENUS	CAS3D	δf	yes	no	12
CAS3D-K	CAS3D	no	no	no	5

TABLE I. Linear perturbative ideal full MHD/kinetic hybrid codes.

While in the first theoretical models the radial extent of the fast particle orbits had not been considered, meanwhile almost all codes consider the full orbit width (FOW). However, the effects of the finite Larmor radius (FLR) of the fast particles still are not commonly accounted for.

code	MHD code	PIC	FOW	FLR	reference
AE3D-K	AE3D	δf	yes	no	9
CKA-EUTERPE	CKA	δf	yes	adaptive (4-32) points	11

TABLE II. Linear perturbative ideal reduced MHD/kinetic hybrid codes.

The non-perturbative MHD/kinetic hybrid codes, such as MEGA[14], and HMGC[15], solve the time-dependent non-linear MHD equations. The fast particles contribute to the plasma pressure and thus influence the evolution of the modes. This contribution is calculated from the non-linear drift- (HMGC) or gyro-kinetic (MEGA) equation for the fast particle species, where the MHD field enters as an external force.

B. Completely gyro-kinetic

There are also completely kinetic codes which solve the gyro-kinetic equations for all ion species and the electrons together with the Poisson equation and Ampères law. The LIGKA code[16] is an eigenvalue solver which uses pre-calculated orbits from the HAGIS code to integrate the kinetic equations.

Furthermore, there are fully kinetic δf- PIC codes solving the time dependent kinetic equations with marker particles but with a consistently evolving field from the solution of the Maxwell equations.

The GYGLES code[17] is two-dimensional in space and uses an ad-hoc equilibrium (see Appendix) while the EUTERPE code[18,19] is able to use a realistic 3D equilibrium generated with the VMEC code[20]. Note, that the EUTERPE code is participating in this benchmark as a part of CKA-EUTERPE hybrid model, as well as a completely gyrokinetic model. The ORB5 code[21,22] is a global PIC code originally developed for turbulence studies, and extended to its multi-species, electromagnetic version.

C. Gyro-fluid approach

The TAEFL code[24] solves the time dependent reduced MHD equations for the bulk plasma plus energetic ions in a tokamak; the fast particle component is introduced through two additional moment equations (for the density and parallel velocity moments) that couple to the

bulk plasma through their perturbed pressure gradient via the momentum balance relation. The fast particle moment equations include Hammett-Perkins[10] closure relations that simulate, in an average sense, the phase-mixing effects resulting in Landau damping/growth. The closure coefficients are obtained through comparison with analytic TAE growth rate models and fits to the plasma dispersion function; development of improved closure relations and higher order moments for this model is a topic of ongoing research. The bulk + fast ion moment model is solved as a fully coupled system so that non-perturbative effects on the Alfvn mode structure and real frequency are retained. FLR effects are introduced into the model using Padé approximations to the Bessel functions, while the FOW effects enter only to lowest order based on a velocity average of passing particle drifts. The equations are solved using Fourier expansions in poloidal/toroidal angle and finite differences in the flux (radius) coordinate. Both initial value and eigensolver solution methods are available, with the eigensolver option used for the results given in this paper.

III. BENCHMARK SETUP

A circular large aspect ratio tokamak ($A = 10$, $R = 10$ m) has been chosen as a test case. This was dictated by restrictions of the participating codes with respect to geometry or numerical properties. The minor radius is $a = 1\,\mathrm{m}$. The profile of the rotational transform is given by $q(r) = 1.71 + 0.16\,(r/a)^2$, and the magnetic field is 3 T in the center (cf. Ref. 17). For the MHD calculations, the equilibria have been calculated using VMEC or with an appropriate Grad-Shafranov solver while GYGLES, ORB5 and HMGC use an ad-hoc equilibrium (see Appendix).

A TAE mode with $m = 10$, 11 and $n = -6$ is calculated in a hydrogen plasma. Note, that with this convention the decomposition of the mode is done as $\sim \mathrm{e}^{\mathrm{i}(m\theta + n\phi)}$. We use a flat density profile for both electrons and ions, i.e. $n_\mathrm{e} = n_\mathrm{i} = 2.0 \cdot 10^{19}\ \mathrm{m}^{-3}$, while $T_\mathrm{e} = T_\mathrm{i} = 1\,\mathrm{keV}$ holds for the electron and ion temperatures. Note that in fully kinetic codes like GYGLES, EUTERPE and ORB5, the electron density is calculated from the quasi-neutrality condition if fast particles are present. In the hybrid codes, where the electron density does not enter explicitly, quasi-neutrality is simply assumed.

The pressure has to be zero at the boundary for an MHD equilibrium code. Therefore the bulk pressure decays towards the edge for the hybrid models: $p(s) = (7.17 \cdot 10^3 - 6.811 \cdot 10^3\, s - 3.585 \cdot 10^2\, s^2)$ Pa with $s = \Psi_\mathrm{tor}/\Psi_\mathrm{tor}(a)$. However, for the kinetic model the bulk

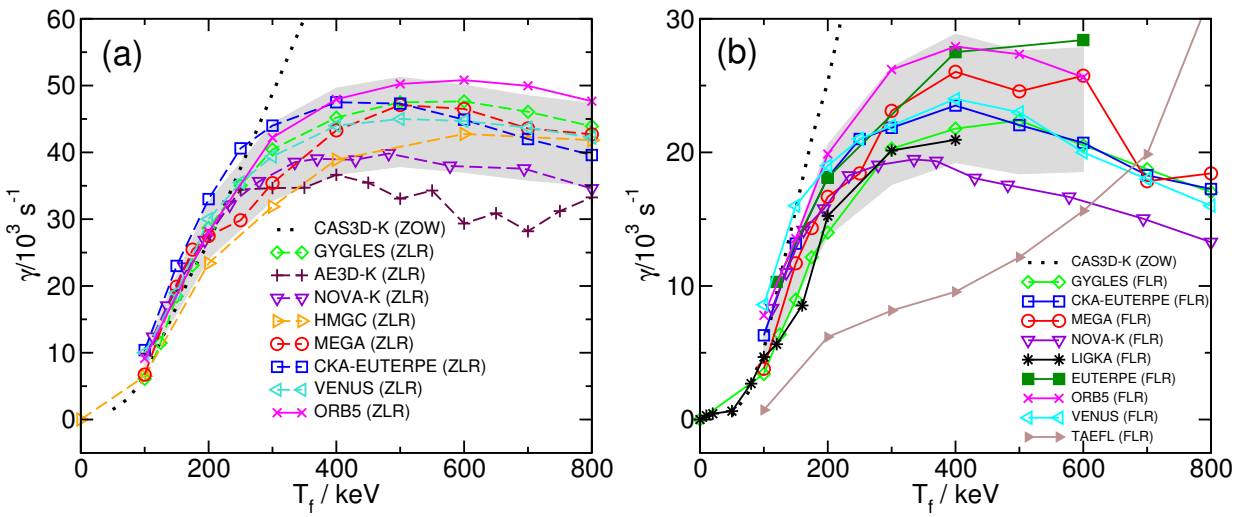

FIG. 1. Growth rates from calculations without FLR effects (a) and with FLR effects (b). The dashed line from CAS3D-K is valid in the limit of zero orbit width (small energies) and is shown for comparison. The shaded grey area marks the ±15% margin around the mean value for (a) and ±20% for (b).

pressure which can be calculated from the background distribution function is taken to be constant to avoid gradient driven modes to become important, i.e. $p(s) = p_\mathrm{i} + p_\mathrm{e} = 6408.0$ Pa. Near the axis the values are quite close and the plasma β is at around 0.2%.

The influence of the fast particle pressure on the equilibrium has not been taken into account in any of the simulations.

The fast particle (deuterons) distribution is taken to be a Maxwellian and is varied in the temperature range from 0 keV to 800 keV. The fast particle density profile is given by

$$n(s) = n_0 c_3 \exp\left(-\frac{c_2}{c_1} \tanh \frac{\sqrt{s} - c_0}{c_2} \right) \tag{1}$$

with $n_0 = 1.44131 \cdot 10^{17}\mathrm{m}^{-3}$ and the coefficients $c_0 = 0.49123$, $c_1 = 0.298228$, $c_2 = 0.198739$, $c_3 = 0.521298$.

IV. RESULTS

A. Frequencies and growth rates

The ideal MHD frequency of the TAE mode found with CAS3D is $\omega = 4.01 \cdot 10^5\,\mathrm{rad\,s^{-1}}$, while $\omega = 4.13 \cdot 10^5\,\mathrm{rad\,s^{-1}}$ has been found with GYGLES. The dominating mode numbers

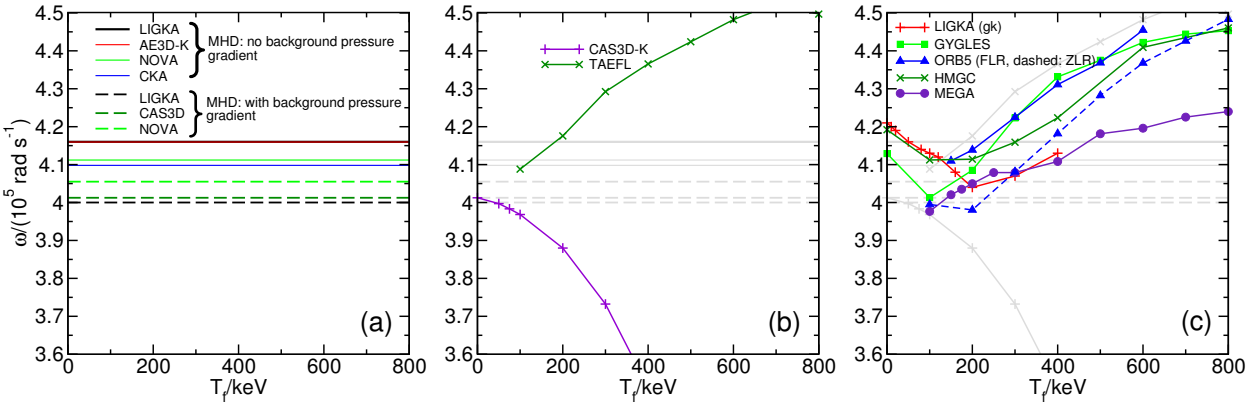

FIG. 2. Results for the modes frequencies:

(a) MHD results which stay constant in perturbative approaches.

(b) Results from CAS3D-K and TAEFL with limited approximation of orbit width and FLR effects.

(c) Results from non-perturbative codes changing the mode frequency by the fast particle pressure.

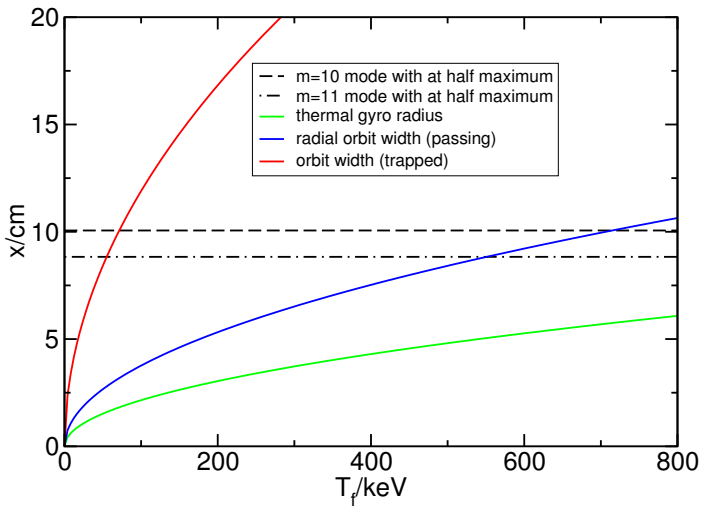

FIG. 3. The size of the thermal gyroradius and the radial orbit width are compared with the width of dominating eigenmode harmonics at half maximum to estimate their importance. The orbit width was calculated using the large aspect ratio estimate[23].

are $m = 10, n = -6$ and $m = 11, n = -6$.

The growth rate has been calculated for different fast ion temperatures. In Fig. 1a the growth rates have been calculated without the effects caused by a finite Larmor radius of the fast ions. Although this limit is appropriate only for small energies, it provides a good comparison as not all participating codes are able to consider FLR effects.

The energy scaling of CAS3D-K can be explained by the missing FOW effects and is shown for comparison.

The growth rates in Fig. 1b are smaller than those without the FLR effects included, but show good agreement among themselves. The gyrofluid model of the TAEFL code gives considerably smaller growth rates at lower energies and deviates strongly from the kinetic

models for higher energies.

Note, that Fig. 1 illustrates only the drive of fast particles implemented in the models. The numerical damping present in the non-perturbative codes and the physical of the fully gyro-kinetic codes are subtracted from the data. So, the comparision is truly that of the included fast particle physics.

To compare the frequencies, the codes have been sorted into three groups. In Figure 2a, there are the MHD results shown which are used by the perturbative codes. These are not changed when the fast particle energy increases as the fast particle pressure does not influence the MHD mode. The results from LIGKA have been obtained in the MHD limit and are shown for comparison. If the background equilibrium pressure is neglected, the MHD mode is somewhat higher than the full MHD result (straight lines compared with dashed). In Figure 2b, the results of those codes are shown which have only a limited account for the orbit width effects. CAS3D-K calculates the frequency response perturbatively and fails to reproduce the rise of the frequency with higher fast particle pressure which is visible in Figure 2c. See Ref. 26 for a discussion and Ref. 17 for similar observations.) Figure 2c collects the results of the most complete physical models including orbit width and FLR effects.

To get an impression when the orbit width reaches the mode width, Fig. 3 compares the thermal gyro radius of the fast particles and large aspect ratio estimates of their orbit width with that of the mode at half maximum. For this case, both, the orbit width as well as the gyro radius are quite large which explains the relatively pronounced effect on growth rates and frequency shifts.

It has been found from analysis of the kinetic MHD results of HMGC and MEGA that the resonances at $v_\mathrm{f}/v_\mathrm{A} = 1/3$ and at $v_\mathrm{f}/v_\mathrm{A} = 1/5$ contribute mostly to the energy transfer between fast particles and waves (Fig. 4).

From our point of view, it was not clear in this field of research how different models would compare with each other. In this light, the relatively large variance of the results for both, FLR and ZLR, is not that surprising. Nevertheless it deserves discussion. One point is certainly that already the frequencies in the MHD limit disagree by around 4%. The same is true for the non-perturbative codes, also here already the frequencies disagree. However, there is no unexpected behavior of the frequency visible. Therefore, it is correct to assume that all codes where addressing the same mode despite their very different models. Judging from the growth rates, the frequency shifts and the little change in the eigenmodes (next

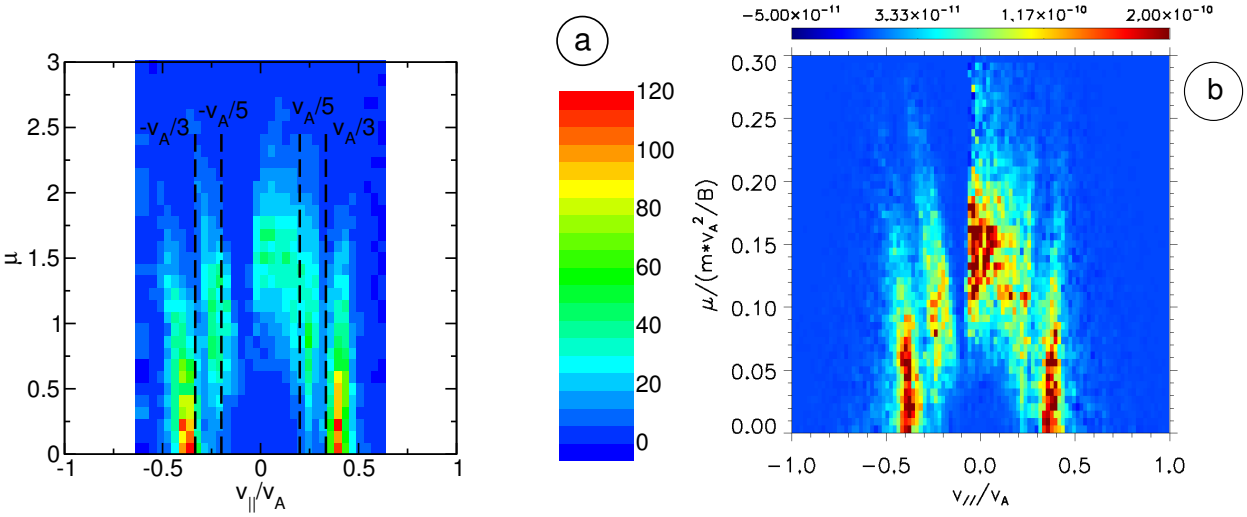

FIG. 4. Spatially averaged energy transfer between waves and the fast particles over velocity space at a given point in time. For HMGC (a) and MEGA (b). The fast particle temperature is 400 keV. In (a), the radial interval considered was $0.448 < s < 0.552$ while for (b) $0 < s < 1$ has been taken.

subsection), the deviation from the MHD result is not large and the case can be treated perturbatively. The remaining sources of error are the different equilibria (ad-hoc, MHD and flat profiles) and numerical differences in the codes.

B. Eigenfunctions

The qualitative agreement between the eigenfunctions is good: Some examples are shown in Fig. 5 and also in Fig. 6 for comparison.

The agreement in the ideal MHD limit (Fig. 5) is very good, especially between the codes which use eigenvalue solvers such as CAS3D, AE3D, CKA, LIGKA and CASTOR. Here, the non-perturbative (time dependent) codes deviate and show a more pronounced side band structure although they have different physical models. This structure, however, might be due to the ad-hoc (without Shafranov shift) equilibrium model used in HMGC and GYGLES.

C. Physical damping mechanisms

The physical damping mechanisms cannot be addressed by all participating codes. Collisional damping can only be calculated by NOVA-K and is found to be $\gamma_{coll} = -0.237 \cdot 10^3 s^{-1}$

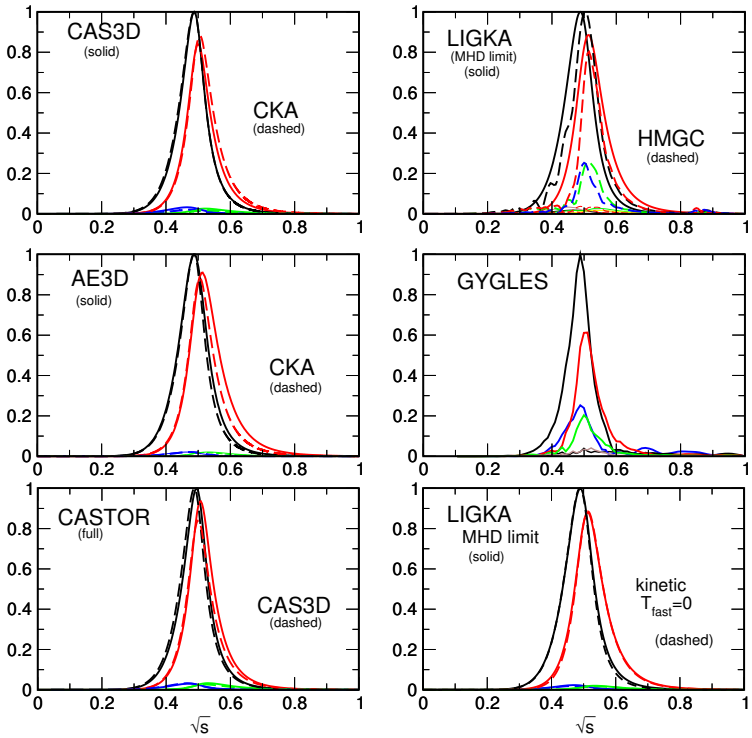

FIG. 5. Eigenfunctions in the ideal MHD limit or the kinetic limit (with kinetic bulk plasma species) without fast particles for $n = -6$. The dashed lines belong to the codename on the right hand side of the figure while the solid lines to that on the left hand side. The color coding is: $m = 10$ - black, $m = 11$ - red $m = 9$ - blue, $m = 12$ - green

for the contribution of the trapped electron population.

Using VENUS for an electron species, the electron Landau damping has been found to be $\gamma_{\mathrm{elLD}} = -1.3 \cdot 10^3 s^{-1}$. All collision-less damping mechanisms of the bulk plasma can only be calculated by the fully gyro-kinetic codes LIGKA, GYGLES and EUTERPE (see Table III). For this calculation, both GYGLES and EUTERPE used the ad-hoc equilibrium.

code	γ/s (co)	γ/s (counter)
LIGKA	-1052	-1517
EUTERPE	-567	-1705
GYGLES	-1103	

TABLE III. Damping rates from gyrokinetic codes

In the GYGLES code, the diagnostics was not been able to distinguish between the two counterpropagating MHD modes. The values agree fairly well, although PIC-codes are routinely plagued with noise issues and the two co-existing MHD modes cause additional numerical problems. Only the δf method together with the elaborated numerical algorithms[17,18] used here allows a quite accurate calculation.

For the comparison with the results of the other codes it must be remembered that the fully kinetic codes consistently include the damping by the bulk plasma. As stated above, the

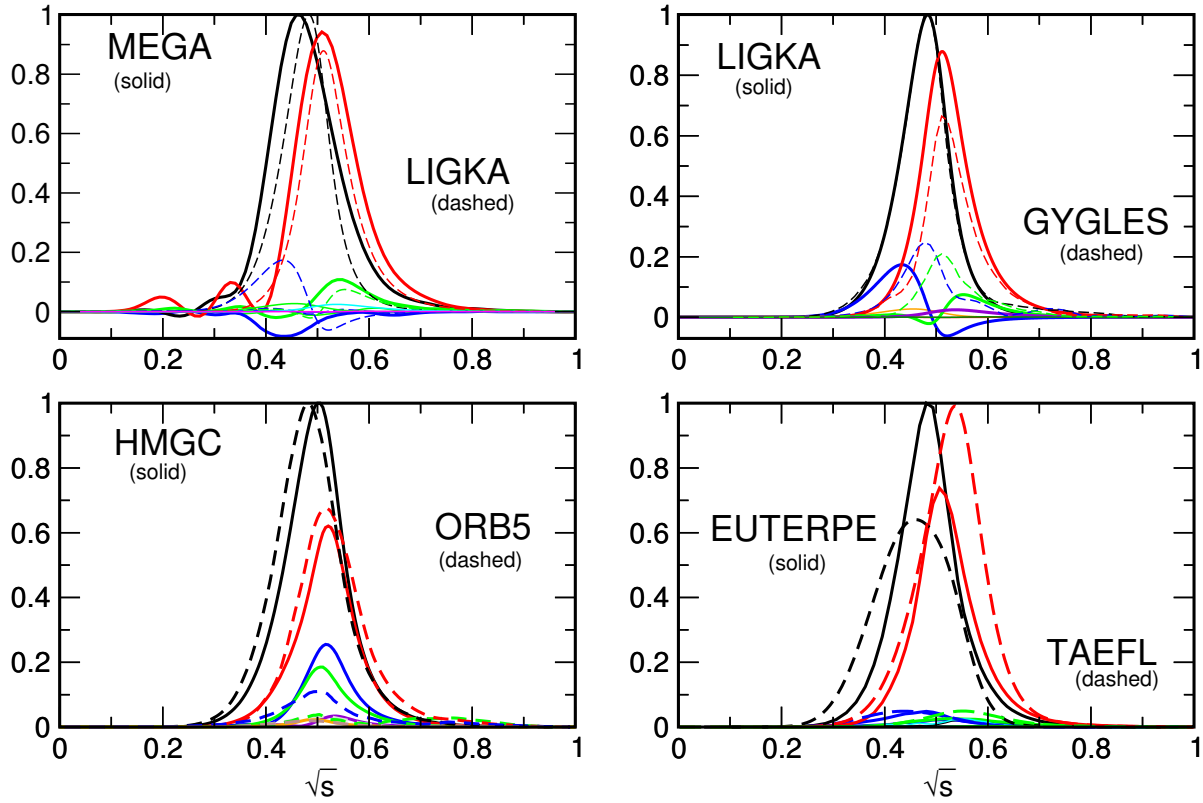

FIG. 6. Eigenfunctions for a fast ion energy of 400 keV. The dashed lines belong to the code- name on the right hand side of the figure. The color coding is as in Fig. 5 For TAEFL, $|\phi|$ is shown.

benchmarks aims to compare the **drive** of fast particles.

We have corrected all growth rates in Fig. 1 by subtracting the respective damping rates (both collisional and collisionless) that were found for each code, so that $\gamma = 0$ for $T_f = 0$. Note that, in some codes (namely MEGA and HMGC), these damping rates depend on T_f. In those cases, the applied correction was also T_f-dependent.

D. Numerical issues and model limitations

1. Proper choice of the distribution function

In the kinetic part of the theory, the initial distribution function of the fast particles has to be chosen such that the distribution function is a function of the constants of motion. This choice guarantees that no relaxation occurs without a perturbation and justifies a linearization of the Vlasov equation.

However, in this work, the distribution function has been chosen to be a function of the flux

label s rather than the toroidal momentum $P_\phi = \frac{q}{c}\Psi_{\rm pol} + mRv_\parallel \frac{B_\phi}{B}$. This was partly due to technical reasons but also because the stellarator codes do not use P_ϕ as it is not conserved in stellarators. Note that with the transition to an analogous distribution function depending on P_ϕ (cf. Ref. 6) the growth rate is smaller by approximately a factor of two (NOVA-K calculation). The terms leading to a relaxation of f_0 have been switched off in all codes.

2. Lost marker particles in δf PIC simulations

Due to their large orbit width, the fast particles may leave the simulation domain. The same is true for the marker particles in PIC simulations.(Please note, that for δf simulations one has to distinguish between marker particles and the weight they carry. The weight is measuring the physical distribution function f.) Having not considered an explicit particle source, lost markers violate the assumptions used to derive the numerical scheme. Here, two heuristic fixes to this problem have been used and compared (Fig. 7). It can be seen that the re-insertion procedure matters for the result and deserves to be explored further as the issue is relevant for other particle following codes as well.
LIGKA pre-caluclates the particles orbit properties on a fixed energy grid. Therefore, at high energies (T > 400 keV) the grid would need to be refined in order to resolve properly the lost-particle boundary that influences significantly the EP drive. This convergence study was not carried out here and therefore no LIGKA results for T > 400 keV are available.

3. Numerical damping in time dependent MHD codes

The non-perbaturbative MHD-kinetic hybrid codes like MEGA and HMGC inherently have numerical damping. This is due to the finite viscosities and resistivities which have to be used in those models to suppress numerical instabilities. Varying the fast particle density in growth rate calculations, the damping value can be extrapolated. The growth rates in this work have been corrected by adding the damping value. Note, that damping rates vary with temperature. For example, for the MEGA code without FLR, the damping rate is $-1.2 \cdot 10^3\,\mathrm{s}^{-1}$ for $T = 200$ keV. and $-4.4 \cdot 10^3\,\mathrm{s}^{-1}$ for $T = 400$ keV. They are comparable to the collisionless damping rate from LIGKA and GYGLES. Of course this agreement is coincidental. Nevertheless, it may explain why MHD/kinetic-hybrid codes can successfully reproduce non-linear saturation levels which depend also on the damping of the mode. A

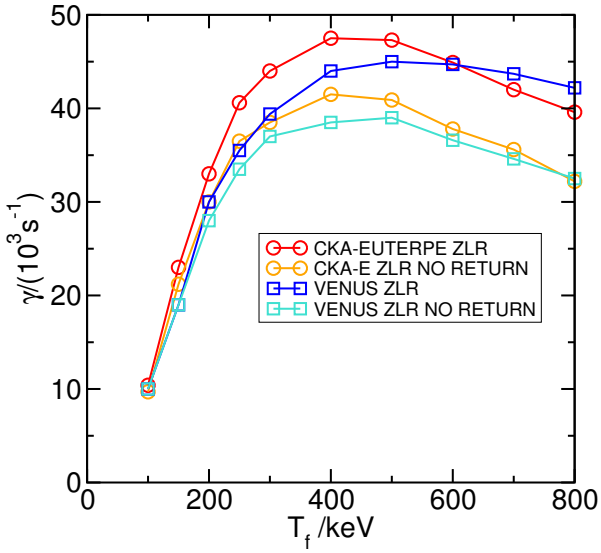

FIG. 7. Two of the hybrid kinetic MHD PIC codes changed the particle return policy between no-return (i.e. the particles which leave the torus are lost and not longer considered) and a procedure where the weight of those particles is set to zero and the particle is re-inserted symmetrically to the midplane.

discussion of the choice of damping parameters can be found in Ref. 27.

V. CONCLUSIONS

A linear benchmark for the calculation of the growth rate of a TAE mode[17] has been performed by a number of codes using fully gyro-kinetic, kinetic MHD and gyro-fluid models. The importance of FLR effects has been illustrated, which is in agreement with earlier research[6]. The MEGA code has been upgraded for this benchmark, to include FLR effects and an extended version of HMGC is under construction[25]. Leaving aside the particular behavior of the gyro-fluid model, the overall agreement of the codes is satisfactory for fast particle energies below 400 keV and lies within $\pm$ 20% for the codes including FLR effects and $\pm$ 15% for those without such effects. The source of the deviations seems to rest in the different physical models used.

The frequency changes with a rising temperature of the fast particles have been investigated for those participating codes which where able to calculate them. It has been found that the models with full orbit width show qualitatively similar behavior. The mode frequency drops for lower fast particle energy and increases as soon as T_f exceeds $100 - 200$ keV.

For higher energies, the orbits become large and numerical problems (lost particles, orbits outside the plasma boundary) become more severe.

With respect to calculations for burning plasmas in large machines the relative effect of the orbit size might be smaller, however the question of lost particles should be addressed in further research.

The results of the paper show that although there is agreement, further code verification is necessary to decrease the deviation of the results. Further code improvements should focus on the inclusion of more physical effects, especially of damping and realistic equilibriums to allow a successful application to ITER.

ACKNOWLEDGEMENTS

This work was in part carried out using the HELIOS supercomputer system at Computational Simulation Centre of International Fusion Energy Research Centre (IFERC-CSC), Aomori, Japan, under the Broader Approach collaboration between Euratom and Japan, implemented by Fusion for Energy and JAEA. Also, some simulations have been performed on the local cluster in Greifswald, where support of Henry Leyh is appreciated.

Finally, the authors would like to thank the anonymous referee for his constructive criticism which helped to improve the quality of the paper.

This work was also partly carried out at the MARCONI supercomputer system of EUROfusion hosted at CINECA in Italy. This work has been partly carried out within the framework of the EUROfusion Consortium and has received funding from the Euratom research and training programme 2014–2018 under grant agreement No 633053. The views and opinions expressed herein do not necessarily reflect those of the European Commission.

REFERENCES

[1]C. Z. Cheng, L. Chen, and M. S. Chance, *Ann. Phys* **161** 21 (1985).

[2]L. Chen and F. Zonca, Rev. Mod. Phys. **88**, 015008 (2016).

[3]ITPA group on energetic particles, D. Borba, A. Fasoli, S. Günter N. N. Gorelenkov, Ph. Lauber, N. Mellet, R. Nazikian, T. Panis, S. D. Pinches, D. Spong, D. Testa, and JET-EFDA contributors, 23st IAEA Fusion Energy Conference, pp. TWP/P708 (2010)

[4]A. Könies, S. Briguglio, N. Gorelenkov, T. Fehér, M. Isaev, P. Lauber, A. Mishchenko,

D. A. Spong, Y. Todo, W. A. Cooper, R. Hatzky, R. Kleiber, M. Borchardt, G. Vlad and ITPA EP TG, "Benchmark of gyrokinetic, kinetic MHD and gyrofluid codes for the linear calculation of fast particle driven TAE dynamics", *IAEA-FEC*, ITR/P1-34 (2012).

[5]A. Könies, A. Mishchenko, and R. Hatzky, Theory of Fusion Plasmas, pp. 133–143 (2008).

[6]N. N. Gorelenkov, C. Z. Cheng, and G. Y. Fu, *Phys. Plasmas* **6**, 28022807 (1999).

[7]S. D. Pinches, L. C. Appel, J. Candy, S. E. Sharapov, H. L. Berk, D. Borba, B. N. Breizman, T. C. Hender, K. I. Hopcraft, G. T. A. Huysmans, W. Kerner, *Computer Physics Communications* 111, 133-149 (1998).

[8]C. Slaby, A. Könies, R. Kleiber, J. M. García-Regaña *Nucl. Fusion* 58, 082018 (2018).

[9]D. Spong, E. D'Azevedo, and Y. Todo, *Contr. Plasma Phys.* **50**, 708712 (2010).

[10]G. W. Hammett, F. W. Perkins, Phys. Rev. Lett., Vol. 64, 3019(1990)

[11]T. Fehér, A. Könies, and R. Kleiber. IAEA TM on Energetic Particles Austin, TX (2011).

[12]W. A. Cooper, J. P. Graves, S. Brunner, and M. Yu. Isaev, *Plasma Phys. Contr. Fusion* **53** 2, 024001 (2011).

[13]A. Y. Aydemir, *Phys. Plasmas* 1, 822 (1994).

[14]Y. Todo and T. Sato, *Phys. Plasmas* **5** 13211327 (1998).

[15]S. Briguglio, et al., *Phys. Plasmas* **2**, 3711 (1995).

[16]Ph. Lauber, S. Günter, A. Könies, and S. D. Pinches, *J. Comp. Phys.* **226**, 447–465 (2007).

[17]A. Mishchenko, A. Könies, and R. Hatzky, *Phys. Plasmas* **16** 8, 082105 (2009).

[18]A. Mishchenko, M. Borchardt, M. Cole, R. Hatzky, T. Fehér, R. Kleiber, A. Könies and A. Zocco *Nuclear Fusion* **55**, 53006 (2015).

[19]R. Kleiber, Theory of Fusion Plasmas, pp. 136146 (2006).

[20]S. P. Hirshman, W. I. van Rij, and P. Merkel, *Comp. Phys. Comm.* **43**, 143-155 (1986).

[21]S. Jolliet, A. Bottino, P. Angelino, R. Hatzky, T. M. Tran, B. F. Mcmillan, O. Sauter, K. Appert, Y. Idomura, and L. Villard, *Comput. Phys* **177**, 409 (2007).

[22]A. Bottino, T. Vernay, B. D. Scott, S. Brunner, R. Hatzky, S. Jolliet, B. F. McMillan, T. M. Tran, and L. Villard *Plasma Phys. Controlled Fusion* **53**, 124027 (2011).

[23]P. Helander and D. J. Sigmar, Collisional Transport in Magnetized Plasmas, Cambridge University Press 2002.

[24]D. Spong, B. Carreras, and C. Hedrick, *Phys. Fluids* **B 4**, 10, 33163328 (1992).

[25]X. Wang, S. Briguglio, L. Chen, C. Di Troia, G. Fogaccia, G. Vlad, and F. Zonca, *Phys. Plasmas* **18**, 052504 (2011).

[26]C. Slaby, A. Könies, R. Kleiber, *Phys. Plasmas* 23, 092501 (2016).

[27]Y. Todo, H. L. Berk, B. N. Breizman *Nucl. Fusion* 50, 084016 (2010).

Appendix A: Ad hoc equilibrium

The ad-hoc equilibrium is a circular tokamak with concentric flux surfaces and is defined by

$$\vec{B} = F(\Psi)\nabla\phi + \nabla\Psi \times \nabla\phi \tag{A1}$$

where Ψ is the poloidal toroidal flux, $F = B_0 R$ and B_0 is the reference magnetic field. In order to complete the specification, we define

$$\frac{\mathrm{d}\Psi}{\mathrm{d}r} = \frac{B_0 r}{\bar{q}(r)} \tag{A2}$$

where $\bar{q}$ is given by the safety factor via $\bar{q}(r) = q(r)\sqrt{1 - (\frac{r}{R})^2}$.